ATMOSPHERIC TURBULENCE MITIGATION BASED ON TURBULENCE EXTRACTION

Renjie He[⋆†] *Zhiyong Wang*[†] *Yangyu Fan*[⋆] *David Feng*[†]

[⋆] Shaanxi Key Laboratory of Information Acquisition and Processing,
School of Electronics and Information, Northwestern Polytechnical University, Xian, China.
[†] School of Information Technologies, The University of Sydney, Australia.

ABSTRACT

A video taken under the influence of atmospheric turbulence suffers from serious distortion caused by the variation of optical refractive index. In order to reduce geometric distortion and time-space-varying blur, and recover both coarse structure and fine details, a novel turbulence extraction based approach for recovering a latent image from an atmospheric turbulence degraded imagery sequence is proposed. Firstly, a non-rigid image registration method is applied as a preprocessing to reduce geometric deformation. Secondly, the registered image sequence is decomposed into a low-rank background scene component and a sparse turbulent component via matrix decomposition. Different from other approaches, which intend to remove turbulence directly, we manage to extract information of distortion position from the sparse turbulent component to indicate the sharpest turbulence patches. The selected sharpest turbulence patches are then enhanced and fused to generate an enhanced detail layer. Finally, the output image is generated by fusing the deblurred background scene layer and the enhanced detail layer together. Experiments indicate that our approach is capable of significantly alleviating atmospheric turbulence blur and geometric distortion.

Index Terms— atmospheric turbulence, image restoration, low-rank decomposition, guided filter.

1. INTRODUCTION

In long range imaging process, an image or video obtained is often suffered from geometric distortion and blur caused by atmospheric turbulence. Influenced by ambient air pressure, temperature, humidity, carbon dioxide level and air dust density, atmospheric turbulence randomly alters the air refraction index along the light transmission path [1] and hence causes shimmering and distortion. Examples of such distortion could be easily observed at positions where the temperature gradients are large, such as hot road surface, deserts, exhausts of jet planes and objects above flame. As shown in Fig. 1, the observed frame (Fig. 1 (a)) is severely deformed and blurred by atmospheric turbulence, compared with the ground truth image (Fig. 1 (b)) [2].

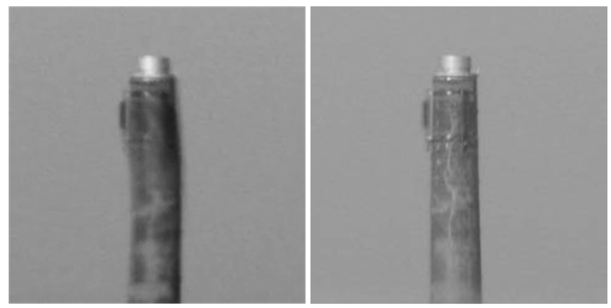

(a) (b)

Fig. 1. A sample of atmospheric turbulence distortion. (a) An observed frame, (b) Ground truth of the scene.

In the situation that the scene and the camera are both static, the imaging process with the degradation caused by atmospheric turbulence can be mathematically modeled as follows:

$$F_k(\mathbf{x}) = D_k(H_k(J(\mathbf{x}))) + n_k(\mathbf{x}), \quad (1)$$

where $k = 1, \ldots, N$ is the frame number. $F(\mathbf{x})$, D and H are the observed image sequence, an operator which indicates the geometric distortions caused by turbulence, and a blur kernel, respectively. $J(\mathbf{x})$ is the ideal error-free image of the scene, which is not subject to blurring and distortion, $n(\mathbf{x})$ is an additive noise. The objective of turbulence mitigation is to estimate $J(\mathbf{x})$ from the observed degraded image sequence $F_k(\mathbf{x})$. However, turbulence mitigation is a challenging task due to its ill-posed nature. Moreover, the amount of turbulence varies both spatially and temporally.

Various approaches have been proposed to mitigate the influence of atmospheric turbulence recent years[1, 2, 3, 4, 5, 6, 7, 8]. In [2], Hirsch *et al.* introduced a Efficient Filter Flow (EFF) technique by dividing each frame into several isoplanatic regions and estimating the PSF separately for each patch through a blind deconvolution algorithm. However, their method is suitable for low geometric distortion situation only and ringing artifacts still exist due to the limita-

This work is partially supported by the Natural Science Foundation of China (No. 61420106007, 61171154).

tion of local PSF estimation. In [8], Oreifej *et al.* proposed to mitigate turbulence and detect moving object simultaneously for tracking objects. They decomposed the turbulence sequence into three components: the background, the turbulence and the object, with a three-term low-rank matrix decomposition. However, their results are not directly comparable to background subtraction or turbulence mitigation approaches. In [9], Anantrasirichai *et al.* proposed to alleviate turbulence by region-level fusion based on the dual tree complex wavelet transform. Their method was able to achieve good performance due to both pre-processing (e.g., region of interest alignment) and post-processing (e.g., contrast enhancement). In [5], Zhu *et al.* extended their previous restoration framework [10] by reducing the variance of spatially and temporally changing PSFs via non-parametric kernel regression. They firstly applied image registration to each frame in order to remove geometric distortion. After that, a single image with only space invariant near-diffraction-limited blur was reconstructed via fusion process.

Though capable of reducing distortion and blur and recovering coarse structure caused by turbulence, the approaches mentioned above still have limitations on restoring fine details. In this paper we propose a novel approach based on turbulence extraction for restoring a single clear image from an observed image sequence degraded by atmospheric turbulence, which is capable of restoring both coarse structure (overall sharpness) and fine details simultaneously.

2. PROPOSED TURBULENCE EXTRACTION BASED APPROACH FOR ATMOSPHERIC TURBULENCE MITIGATION

As mentioned above that both the scene and the camera are static, therefore, the corresponding part in each frame of the observed sequence are linearly correlated to some degree. Based on this rationale, the observed sequence can thus be decomposed into a low-rank scene component and a sparse turbulent component.

However, in the situation that the deformation is large, the linear correlationship of the sequence matrix may be unavailable. In order to reduce the effect of the spatially and temporally varying deformation, we first apply a B-spline based non-rigid registration on the observed sequence as a pre-processing. After that, in order to separate the static scene object and the varying turbulence, we utilize a matrix decomposition approach. We restore fine details from the obtained sparse turbulent component using novel enhancement and fusion methods. Meanwhile, we restore coarse structure information from the low rank scene component using a blind deconvolution method. Finally, the restored image is obtained by fuse the enhanced detail layer and the low rank background scene together. Details of each step are described in following subsections.

2.1. Image Registration

Since the linear correlationship of the sequence matrix may be unavailable if the geometric deformation varies dramatically. Image registration technique is first applied as a pre-processing to suppress the geometric deformation.

The geometric deformation caused by turbulence can be considered as a non-rigid transformation between each observed frame and the scene [1]. Therefore, the turbulent deformation can be expressed using a non-rigid motion model by manipulating an equally spaced control grid P overlaid on a fixed reference image J. In [3], *Zhu et al.* introduced a more natural symmetry constraint into the B-spline registration algorithm based on the important property that the registration should be symmetric or inverse consistent [11, 12]. In this paper, we directly utilize the B-spline based registration technique proposed in [3] to generate the the registered sequence $\{R_k\}$.

2.2. Turbulence Extraction

After the registration, according to the prior knowledge that scene and camera are both static, the matrix of scene component is assumed to be low-rank, and the differences of each frame can be considered as sparse noise. Inspired by the approach described in [13], in order to extract these noise, we apply rank minimization to decompose the registered image sequence $\{R_k\}$ into a fixed low rank background scene R^L and a set of sparse error $\{R_k^S\}$. By stacking pixels of each registered frames into a column vector, we can obtain a frame matrix $R = [vec\{R_1\}, \dots, vec\{R_N\}]$, where $vec : \mathbb{R}^{w\times h} \to \mathbb{R}^L$ denotes the stacking operator. The decomposition can be modelled as:

$$\begin{cases} \min\limits_{B,S} Rank(B) \text{ s.t. } R = B + S, \\ \qquad \|S\|_F \leq \sigma, \end{cases} \tag{2}$$

where $S = \left[vec\{R_1^S\}, \dots, vec\{R_N^S\}\right]$ is the sparse error matrix, and $B = \left[vec\{R_1^L\}, \dots, vec\{R_N^L\}\right]$ is the low rank background scene matrix. $\|\bullet\|_F$ is the Frobenius norm and σ is a constant that represents the maximum total variance of corrupted pixels across all images [14].

Since it is difficult to optimize (2) directly, we rewrite the equation by applying a convex relaxation according to [15]. Consequently, the Lagrange form of (2) can be rewritten as follows:

$$\min_{B,S} \|B\|_* + \gamma \|S\|_F^2 \text{ s.t. } R = B + S, \tag{3}$$

where γ is a positive weighting parameter, $\|\bullet\|_*$ is the nuclear norm indicating the sum of all singular values.

The Augmented Lagrange Multiplier (ALM) algorithm [14] is utilized in our paper to solve this problem. After matrix decomposition, a fixed low-rank background scene image sequence $\{R_k^L\}$ and a sparse noise sequence $\{R_k^S\}$ can be extracted from B and S, respectively.

2.3. Fine Detail Restoration

In order to restore fine details, we propose a patch selection and fusion based method. It is observed in the left image of Fig. 2 that sequence $\{R_k^S\}$ contains position information of distortions which could be utilized for distortion estimation. Moreover, each frame in $\{R_k^S\}$ also contains local Gaussian-like noise which could be removed by averaging process. The image on the right of Fig. 2 shows the averaging result of $\{R_k^S\}$, which is denoted as $\bar{R}^S(\mathbf{x})$. As shown in the figure, although $\bar{R}^S(\mathbf{x})$ is still blurry, it provides a good estimation of positions where the scene was distorted by turbulence.

As mentioned in [16, 17], for short-exposure images, turbulence creates random appearance of high quality regions. In order to obtain these regions, we first create a binary image from $\bar{R}^S(\mathbf{x})$ using adaptive thresholding method. Denote the binarized $\bar{R}^S(\mathbf{x})$ as $\bar{R}^{BW}(\mathbf{x})$ and local patches centred at each 1-valued pixel of $\bar{R}^{BW}(\mathbf{x})$ as Ω^i_{BW}, where $i = 1, \ldots, M$ and M is the total patch number. In this paper, we test with different patch sizes and finally set the patch size to 31×31 experimentally. In addition, we denote patches with the same position of Ω^i_{BW} in $\{R_k\}$ as Ω^i_k, where $k = 1, \ldots, N$ is the frame index. Obviously, there would be M patches for each frame in $\{R_k\}$.

In order to select the sharpest i-th patch, denoted as $\hat{\Omega}^i$, within N corresponding patches $\{\Omega^i_k | k = 1, ..., N\}$, we detect local sharpness and similarity to the local patch mean for each corresponding patch through all registered frames.

Fig. 3 illustrates the patch selection process. As shown in the figure, the red rectangle box in the left frame shows a patch Ω^i_{BW} in $\bar{R}^{BW}$. In order to pick out the corresponding patch with the best quality, we compare corresponding patches $\{\Omega^i_k | k = 1, ..., N\}$ in $\{R_k\}$ and select the sharpest patch as $\hat{\Omega}^i$. Specifically, as shown in Fig. 3, patch in the k-th frame is selected as $\hat{\Omega}^i$.

With all M patches selected, we further fuse all selected sharp patches $\hat{\Omega}^i$ together to generate a detail layer. However, as $\bar{R}^{BW}$ is not smooth and not aligned with object boundaries, using corresponding patches in $\bar{R}^{BW}$ as fusion weight map directly may produce artifacts to the fused image. In addition, details in $\hat{\Omega}^i$ also need to be enhanced. Inspired by [18], we refine $\bar{R}^{BW}$ and enhance $\hat{\Omega}^i$ using guided image filter.

In our approach, in order to obtain refined weighted patches for detail fusion, a guided filter on each patch Ω^i_{BW} under the guidance of the corresponding sharpest patch of registered image $\hat{\Omega}^i$ is applied as follows:

$$W^i = H_G(\Omega^i_{BW}, \hat{\Omega}^i), \tag{4}$$

where W^i is the output refined patch and H_G denotes the guided filtering operation.

In order to extract details from each patch, we further enhance each selected patch using guided filter. As an image can be modelled as the combination of a smooth layer and a detail layer, image details can be extracted by amplifying the

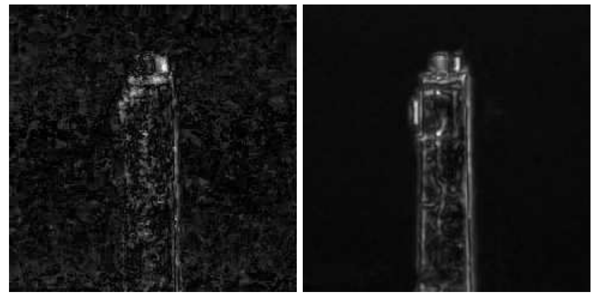

Fig. 2. Result of averaging the sparse turbulent. Left: one frame of turbulent component. Right: averaged turbulent image.

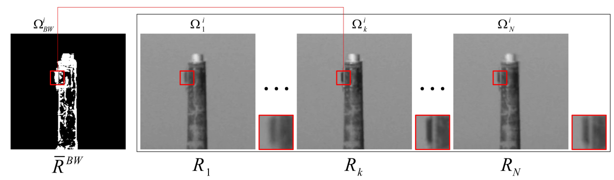

Fig. 3. Illustration of patch selection.

detail layer [19]. In our case, the smooth layer of patch $\hat{\Omega}^i$ can be obtained using guided filter as follows:

$$\hat{\Omega}^i_{\text{smooth}} = H_G(\hat{\Omega}^i, \hat{\Omega}^i), \tag{5}$$

Therefore, details in each patch $\hat{\Omega}^i$ can be enhanced as follows:

$$\hat{\Omega}^i_{\text{enhanced}} = \hat{\Omega}^i_{\text{smooth}} + \tau \left(\hat{\Omega}^i - \hat{\Omega}^i_{\text{smooth}} \right), \tag{6}$$

where τ is a coefficient to control the amplification level and is set to 1.7 experimentally in this paper.

Finally, an enhanced detail layer is fused using weighted averaging:

$$L^D = \sum_{i=1}^{M} W^i \hat{\Omega}^i_{\text{enhanced}}. \tag{7}$$

2.4. Coarse Structure Restoration

In the last step, we apply single image blind deconvolution on background scene $R^L(\mathbf{x})$ to suppress the blurring effect caused by an unknown blur kernel and to restore the coarse structure. Generally, degradation caused by blur can be described as follows:

$$G = F \otimes h + n, \tag{8}$$

where G and F are a blurred image and an unknown sharp image, respectively. h represents the PSF and $\otimes$ indicates convolution operation.

We utilize a total variation (TV) based optimization algorithm [20] in our study for deconvolution, which can be described as follows:

$$\left\langle \hat{F}, \hat{h} \right\rangle = \underset{F,h}{\arg\min} \frac{\mu}{2} \|F \otimes h - G\|^2 + \|\mathbf{D}F\|_1, \qquad (9)$$

where μ is a regularization parameter, $\|\mathbf{D}F\|_1$ is TV norm. Operator $\mathbf{D}$ is a collection of spatial sub-operators. After the above problem is solved iteratively, the final output can be obtained.

We further fuse the deblurred background scene and the enhanced detail layer together using guided filter mentioned above. We show the final results in Fig. 4.

3. EXPERIMENTAL RESULTS

In this section, we present the experimental validation of the proposed restoration approach, with comparison with representative state-of-art approaches: NDL [5], EFF [2] and CLEAR [9]. We employ the video sequence *chimney* for result comparison. The sequence consists of 100 frames and exposure time for each frame is 1/250s. In addition, three full reference image quality metrics, Peak signal to noise ratio (PSNR), perception-based image model (PIM) [21] and multi-scale structural similarity (MSSSIM) [22], are utilized to quantitatively evaluate the performance of the comparison.

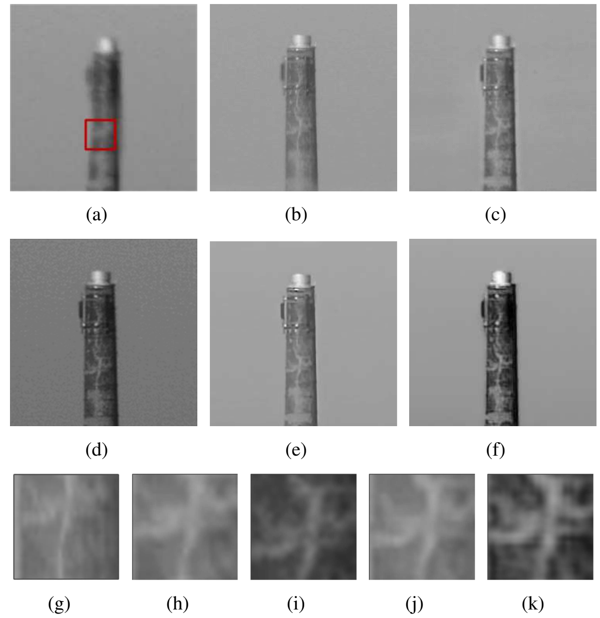

Fig. 4. Comparison results with *Chimney*. (a) An observed frame. (b) Ground truth. (c) EFF's result [2]. (d) CLEAR's result [9]. (e) NDL's result [5]. (f) Our result. (g) Enlarged result of (b). (h) Enlarged result of (c). (i) Enlarged result of (d). (j) Enlarged result of (e). (k) Enlarged result of (f).

Table 1. Quantitative evaluation for *Chimney* (Fig. 4)

	EFF	CLEAR	NDL	Our's
PSNR(dB)	34.46	35.86	35.24	36.05
PIM	35.32	35.71	35.57	35.81
MSSSIM	0.92	0.98	0.95	0.98

Fig. 4 shows the comparison results on *Chimney* . It is observed that geometric deformation is effectively alleviated using each method. Specifically, it is observed in Fig. 4 (a) that, compared with the ground truth image, the obtained frame is severely distorted by turbulence. As observed in Fig. 4 (c), EFF [2] is capable of recovering details faithfully. However, it is noticed that halo artifacts appeared in edge regions. As observed in Fig. 4 (d), result using CLEAR [9] is also visually satisfactory. It is also noticed that result using CLEAR [9] has better contrast because of the contrast enhancement process is applied. However, noise still exists in background. As observed in Fig. 4 (e), NDL [5] produces sharp result around structural areas. However, texture details are lost in their result. As observed in Fig. 4 (f), our result also provides satisfactory restoration result. In addition, as shown in the right-bottom corner of enlarged results corresponding to the red rectangle of Fig. 4 (a), it is also observed that our result has better performance on detail preservation, veins on the chimney become visible.

Table 1 shows the quantitative evaluation on database *Chimney*. It is observed that in Table 1, our approach has the best quality index compared with EFF, CLEAR and NDL. It is noticed that CLEAR also has the highest value of MSSSIM due to the contrast enhancement as post processing.

4. CONCLUSION

In this paper, we present a novel approach for mitigating the atmospheric turbulence caused degradation by extracting turbulence component. We firstly applied a non-rigid registration method to correct geometric distortion from the observed imagery sequence. After that, we decompose the registered image sequence into a low-rank background scene image and a sparse noise sequence. In addition, we select the sharpest patch in registered images at position provided by averaging the sparse noise sequence. Each sharp patch is then enhanced and fused together to produce a enhanced detail layer using guided image filter. After applying blind deconvolution to background scene image, we fuse the deblurred background scene and enhanced detail layer together to generate the final output. Both qualitative and quantitative experimental results demonstrate that our proposed approach can effectively remove the distortion and blur caused by turbulence.

5. REFERENCES

[1] M Shimizu, S Yoshimura, M Tanaka, and M Okutomi, "Super-resolution from image sequence under influence of hot-air optical turbulence," in *Proc. IEEE Conf. Comput. Vision Pattern Recognit.*, Anchorage, USA, Jun. 2008, pp. 1–8.

[2] Michael Hirsch, Suvrit Sra, Bernhard Scholkopf, and Stefan Harmeling, "Efficient filter flow for space-variant multiframe blind deconvolution," in *Proc. IEEE Conf. Comput. Vision Pattern Recognit.*, San Francisco, USA, Jun. 2010, pp. 607–614.

[3] Xiang Zhu and Peyman Milanfar, "Image reconstruction from videos distorted by atmospheric turbulence," in *Proc. SPIE Int. Soc. Opt. Eng.*, San Jose, USA, Jan. 2010, pp. 1–8.

[4] Jérôme Gilles, Tristan Dagobert, and Carlo De Franchis, "Atmospheric turbulence restoration by diffeomorphic image registration and blind deconvolution," in *Proc. Int. Conf. Adv. Concepts Intell. Vis. Syst.*, Juan-les-Pins, France, Oct. 2008, pp. 400–409.

[5] Xiang Zhu and Peyman Milanfar, "Removing atmospheric turbulence via space-invariant deconvolution," *IEEE Trans. Pattern Anal. Mach. Intell.*, vol. 35, no. 1, pp. 157–170, Jan. 2013.

[6] K.B. Gibson and T.Q. Nguyen, "An analysis and method for contrast enhancement turbulence mitigation," *IEEE Trans. Image Process.*, vol. 23, no. 7, pp. 3179–3190, Jul. 2014.

[7] Dalong Li, Russell M Mersereau, and Steven Simske, "Atmospheric turbulence-degraded image restoration using principal components analysis," *IEEE Geosci. Remote Sens. Lett.*, vol. 4, no. 3, pp. 340–344, Jul. 2007.

[8] O Oreifej, Xin Li, and M Shah, "Simultaneous video stabilization and moving object detection in turbulence," *IEEE Trans. Pattern Anal. Mach. Intell.*, vol. 35, no. 2, pp. 450–462, Feb. 2013.

[9] N Anantrasirichai, A Achim, N Kingsbury, and D Bull, "Atmospheric turbulence mitigation using complex wavelet-based fusion," *IEEE Trans. Image Process.*, vol. 22, no. 6, pp. 2398–2408, Jun. 2013.

[10] Xiang Zhu and Peyman Milanfar, "Stabilizing and deblurring atmospheric turbulence," in *Proc. IEEE Int. Conf. Comput. Photogr.*, Pittsburgh, USA, Apr. 2011, pp. 1–8.

[11] Sina Farsiu, Michael Elad, and Peyman Milanfar, "Constrained, globally optimal, multi-frame motion estimation," in *Proc. IEEE Workshop Stat. Signal Process.*, Novosibirsk, Russia, Jul. 2005, pp. 1396–1401.

[12] Mirza Faisal Beg and Ali Khan, "Symmetric data attachment terms for large deformation image registration," *IEEE Trans. Med. Imaging*, vol. 26, no. 9, pp. 1179–1189, Sep. 2007.

[13] Omar Oreifej, Guang Shu, Teresa Pace, and Mubarak Shah, "A two-stage reconstruction approach for seeing through water," in *Proc. IEEE Conf. Comput. Vision Pattern Recognit.*, Colorado Springs, USA, Jun. 2011, pp. 1153–1160.

[14] Zhouchen Lin, Minming Chen, and Yi Ma, "The augmented lagrange multiplier method for exact recovery of corrupted low-rank matrices," Uilu-eng-09-2215, Univ. of Illinois at Urbana-Champaign, 2009.

[15] Emmanuel J Candès, Xiaodong Li, Yi Ma, and John Wright, "Robust principal component analysis?," *J. ACM*, vol. 58, no. 3, pp. 1–37, May 2011.

[16] Mathieu Aubailly, Mikhail A. Vorontsov, Gary W. Carhart, and Michael T. Valley, "Automated video enhancement from a stream of atmospherically-distorted images: the lucky-region fusion approach," in *Proc. SPIE Int. Soc. Opt. Eng.*, San Diego, USA, Aug. 2009, pp. 1–10.

[17] David L Fried, "Probability of getting a lucky short-exposure image through turbulence," *J. Opt. Soc. Am.*, vol. 68, no. 12, pp. 1651–1657, Dec. 1978.

[18] Kaiming He, Jian Sun, and Xiaoou Tang, "Guided image filtering," *IEEE Trans. Pattern Anal. Mach. Intell.*, vol. 35, no. 6, pp. 1397–1409, Jun. 2013.

[19] Fei Kou, Weihai Chen, Zhengguo Li, and Changyun Wen, "Content adaptive image detail enhancement," *IEEE Signal Process. Lett.*, vol. 22, no. 2, pp. 211–215, Feb. 2015.

[20] Stanley H Chan, Ramsin Khoshabeh, Kristofor B Gibson, Philip E Gill, and Truong Q Nguyen, "An augmented lagrangian method for total variation video restoration," *IEEE Trans. Image Process.*, vol. 20, no. 11, pp. 3097–3111, Nov. 2011.

[21] Fan Zhang and David R Bull, "A parametric framework for video compression using region-based texture models," *IEEE J. Sel. Top. Signal Process.*, vol. 5, no. 7, pp. 1378–1392, Nov. 2011.

[22] Zhou Wang, Eero P Simoncelli, and Alan C Bovik, "Multiscale structural similarity for image quality assessment," in *Proc. IEEE Asilomar Conf. Signals, Syst., Comput.*, Pacific Grove, USA, Nov. 2003, pp. 1398–1402.